

Correlation between Structural and Solution Calorimetric Data for Cp*Ru(PR₃)₂Cl (Cp* = C₅Me₅) Complexes

Dale C. Smith, Jr., Christopher M. Haar, Lubin Luo, Chunbang Li, Michèle E. Cucullu, Charles H. Mahler,[†] and Steven P. Nolan*

Department of Chemistry, University of New Orleans, New Orleans, Louisiana 70148

William J. Marshall, Nancy L. Jones,[‡] and Paul J. Fagan

Central Research and Development Department, E. I. DuPont de Nemours & Co., Inc., Experimental Station, P.O. Box 80328, Wilmington, Delaware 19880-0328

Received February 11, 1999

Single-crystal X-ray diffraction studies were conducted on the following compounds: Cp*Ru(PMe₃)₂Cl (**1**), Cp*Ru(PPhMe₂)₂Cl (**2**), Cp*Ru(PMePh₂)₂Cl (**3**), Cp*Ru(PPh₃)₂Cl (**4**), Cp*Ru(PET₃)₂Cl (**5**), Cp*Ru(AsEt₃)₂Cl (**6**), Cp*Ru(PⁿBu₃)₂Cl (**7**), and Cp*Ru(dmpm)Cl (**8**). Structural information obtained from these X-ray studies can be correlated with enthalpies of ligand substitution previously determined from solution calorimetry. The cone angle of the phosphine ligand (monodentate) and the Ru–P bond distance were found to be proportional to the enthalpy of reaction.

Introduction

Thermochemical measurements have been applied for some time to the quantitative assessment of metal–ligand interactions in organometallic systems.¹ We have been investigating the steric and electronic contributions present in tertiary phosphine and arsine-based organoruthenium,² organorhodium,³ and organoiron⁴ systems by means of solution calorimetry. Recent ther-

mochemical studies have determined the enthalpy of reaction values for a series of organoruthenium species⁵ formed in the general reaction depicted in eq 1.



Cp* = C₅(CH₃)₅; COD = cyclooctadiene; L = ER₃ (E = As, P) or L₂ = bidentate phosphine

From this study it was found that the thermochemical trends in this system can be analyzed in terms of a predominant contribution from the Tolman cone angle⁶ of the incoming ligand. We therefore wondered if the same trends were present in metrical parameters obtained from single-crystal X-ray diffraction analysis of the compounds formed in the prior investigation. This paper discusses the correlation between the enthalpies of ligand substitution with metrical parameters determined from single-crystal X-ray diffraction studies of the following eight complexes: Cp*Ru(PMe₃)₂Cl (**1**), Cp*Ru(PPhMe₂)₂Cl (**2**), Cp*Ru(PMePh₂)₂Cl (**3**), Cp*Ru(PPh₃)₂Cl (**4**), Cp*Ru(PET₃)₂Cl (**5**), Cp*Ru(AsEt₃)₂Cl (**6**), Cp*Ru(PⁿBu₃)₂Cl (**7**), and Cp*Ru(dmpm)Cl (**8**).

Results and Discussion

All Cp*RuCl(L)₂ compounds have a central ruthenium atom coordinated by four groups: Cp*, Cl, and the two

* To whom correspondence should be addressed. E-mail: snolan@uno.edu.

[†] Permanent address: Lycoming College, Department of Chemistry, Williamsport, PA 17701.

[‡] Permanent address: LaSalle University, Department of Chemistry and Biochemistry, Philadelphia, PA 19141.

(1) (a) Nolan, S. P. *Bonding Energetics of Organometallic Compounds*. In *Encyclopedia of Inorganic Chemistry*; King, R. B., Ed.; Wiley: New York, 1994. (b) Hoff, C. D. *Prog. Inorg. Chem.* **1992**, *40*, 503–561. (c) Martinho Simões, J. A.; Beauchamp, J. L. *Chem. Rev.* **1990**, *90*, 629–688. (d) Marks, T. J., Ed. *Bonding Energetics in Organotransition Metal Compounds*; ACS Symp. Ser. 428; American Chemical Society: Washington, DC, 1990. (e) Marks, T. J., Ed. *Bonding Energetics in Organotransition Metal Compounds*. *Polyhedron* **1988**, *7*. (f) Skinner, H. A.; Connor, J. A. In *Molecular Structure and Energetics*; Liebman, J. F., Greenberg, A., Eds.; VCH: New York, 1987; Vol. 2, Chapter 6.

(2) For organoruthenium systems see: (a) Li, C.; Serron, S.; Nolan, S. P. *Organometallics* **1996**, *15*, 4020–4029. (b) Serron, S. A.; Luo, L.; Li, C.; Cucullu, M. E.; Nolan, S. P. *Organometallics* **1995**, *14*, 5290–5297. (c) Serron, S. A.; Nolan, S. P. *Organometallics* **1995**, *14*, 4611–4616. (d) Luo, L.; Li, C.; Cucullu, M. E.; Nolan, S. P. *Organometallics* **1995**, *14*, 1333–1338. (e) Cucullu, M. E.; Luo, L.; Nolan, S. P.; Fagan, P. J.; Jones, N. L.; Calabrese, J. C. *Organometallics* **1995**, *14*, 289–296. (f) Luo, L.; Zhu, N.; Zhu, N.-J.; Stevens, E. D.; Nolan, S. P.; Fagan, P. J. *Organometallics* **1994**, *13*, 669–675. (g) Li, C.; Cucullu, M. E.; McIntyre, R. A.; Stevens, E. D.; Nolan, S. P. *Organometallics* **1994**, *13*, 3621–3627. (h) Luo, L.; Nolan, S. P. *Organometallics* **1994**, *13*, 4781–4786. (i) Luo, L.; Fagan, P. J.; Nolan, S. P., *Organometallics* **1993**, *12*, 4305–4311. (j) Nolan, S. P.; Martin, K. L.; Stevens, E. D.; Fagan, P. J. *Organometallics* **1992**, *11*, 3947–3953.

(3) For organoiron systems see: (a) Li, C.; Stevens, E. D.; Nolan, S. P. *Organometallics* **1995**, *14*, 3791–3797. (b) Li, C.; Nolan, S. P. *Organometallics* **1995**, *14*, 1327–1331. (c) Luo, L.; Nolan, S. P. *Inorg. Chem.* **1993**, *32*, 2410–2415. (d) Luo, L.; Nolan, S. P. *Organometallics* **1992**, *11*, 3947–3951.

(4) For organorhodium systems see: (a) Haar, C. M.; Huang, J.; Nolan, S. P. *Organometallics* **1998**, *17*, 5018–5024. (b) Huang, J.; Haar, C. M.; Nolan, S. P.; Marshall, W. J.; Moloy, K. G. *J. Am. Chem. Soc.* **1998**, *120*, 7806–7815. (c) Serron, S.; Nolan, S. P.; Moloy, K. G. *Organometallics* **1996**, *15*, 534–539.

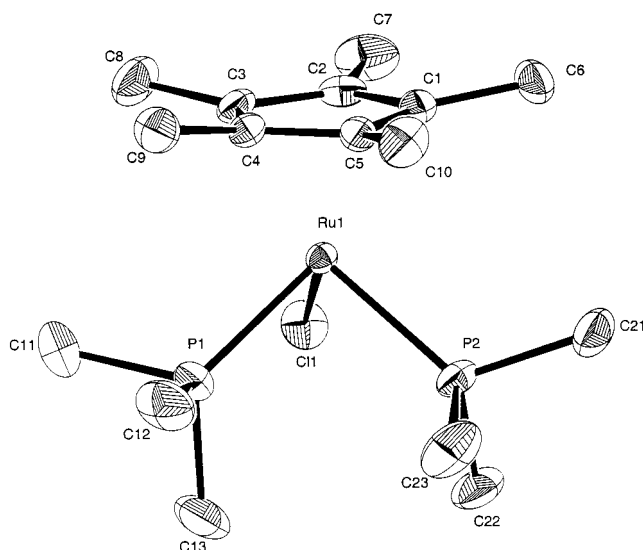
(5) Luo, L.; Nolan, S. P.; Fagan, P. J. *Organometallics* **1993**, *12*, 4305–4311.

(6) (a) Tolman, C. A. *Chem. Rev.* **1977**, *77*, 313–348. (b) Manzer, L. E.; Tolman, C. A. *J. Am. Chem. Soc.* **1975**, *97*, 1955–1956. (c) Tolman, C. A.; Reutter, D. W.; Seidel, W. C. *J. Organomet. Chem.* **1976**, *117*, C30–C33.

Table 1. Enthalpies of Substitution for $\text{Cp}^*\text{Ru}(\text{COD})\text{Cl} + 2\text{L} \rightarrow \text{Cp}^*\text{Ru}(\text{L})_2\text{Cl} + \text{COD}$

complex	L	ΔH_{rxn}^a (kcal/mol)	complex	L	ΔH_{rxn}^a (kcal/mol)
1	PMe_3	-32.2(4)	5	PEt_3	-27.2(2)
2	PPhMe_2	-31.8(3)	6	AsEt_3	-15.0(2)
3	MePh_2	-29.4(2)	7	P^nBu_3	-26.0(2)
4	PPh_3	-22.9(4)	8	dmpm	-33.8(3)

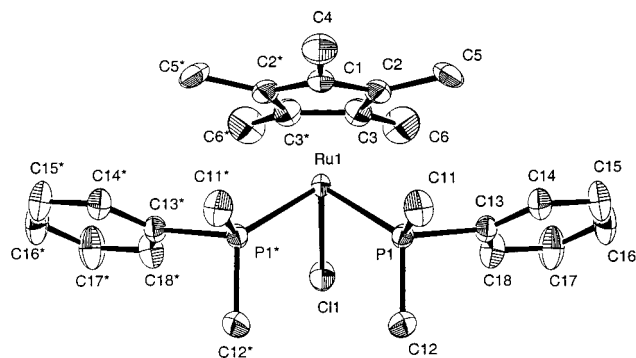
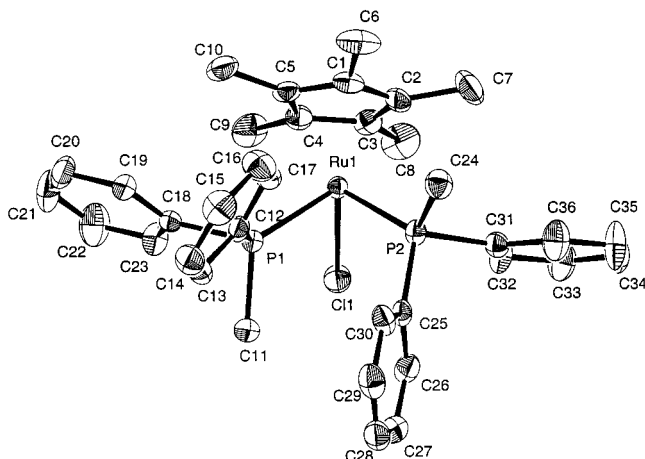
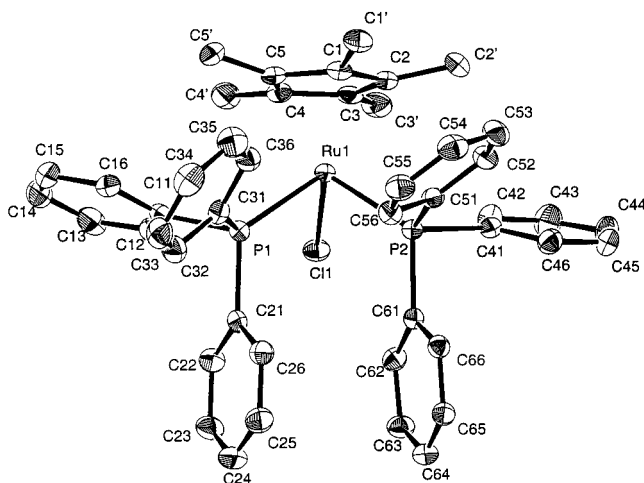
^a Enthalpy values are provided with 95% confidence limits.

**Figure 1.** ORTEP diagram of $\text{Cp}^*\text{Ru}(\text{PMe}_3)_2\text{Cl}$ (**1**) with ellipsoids drawn at 30% probability.

pnictide atoms (either as two separate monodentate ligands or as the two coordinating atoms of a bidentate chelate). Therefore, any variation in structures should be attributed chiefly to the steric and electronic effects of the pnictide ligand(s). In each case, the enthalpy of ligand substitution in the reaction leading to formation of the product has been reported and is summarized in Table 1.⁵

Solid-State Structures of $\text{Cp}^*\text{Ru}(\text{PMe}_3)_2\text{Cl}$ (1**), $\text{Cp}^*\text{Ru}(\text{PPhMe}_2)_2\text{Cl}$ (**2**), $\text{Cp}^*\text{Ru}(\text{PMePh}_2)_2\text{Cl}$ (**3**), and $\text{Cp}^*\text{Ru}(\text{PPh}_3)_2\text{Cl}$ (**4**).** Complexes **1–4**⁷ differ only in the number of phenyl (C_6H_5) and methyl (CH_3) groups on the phosphine ligands. As expected, complexes **1**, **3**, and **4** crystallized in centrosymmetric space groups; $\text{Cp}^*\text{Ru}(\text{PPhMe}_2)_2\text{Cl}$ (**2**), however, crystallizes in the acentric space group $Cmc2_1$ (No. 36), indicating that the compound in the crystal is an optically pure enantiomorph. The absolute configuration of **2** was assigned to the enantiomorph which yielded the lowest R value during least-squares refinement (see Experimental Section). The ORTEP depictions of **1–4** are respectively given in Figures 1–4. Bond distances and angles are given in Table 2.

Average Ru–P bond distances increase in the order **1** < **2** < **3** < **4** (2.293, 2.297, 2.310, 2.342 Å), while the Ru–Cl distances for these complexes are nearly identical. The Ru–P distances in **1–4** are consistent with the electron-donor properties of phosphine ligands and previously determined trends in the enthalpies of ligand

**Figure 2.** ORTEP diagram of $\text{Cp}^*\text{Ru}(\text{PPhMe}_2)_2\text{Cl}$ (**2**) with ellipsoids drawn at 30% probability.**Figure 3.** ORTEP diagram of $\text{Cp}^*\text{Ru}(\text{PMePh}_2)_2\text{Cl}$ (**3**) with ellipsoids drawn at 30% probability.**Figure 4.** ORTEP diagram of $\text{Cp}^*\text{Ru}(\text{PPh}_3)_2\text{Cl}$ (**4**) with ellipsoids drawn at 30% probability.

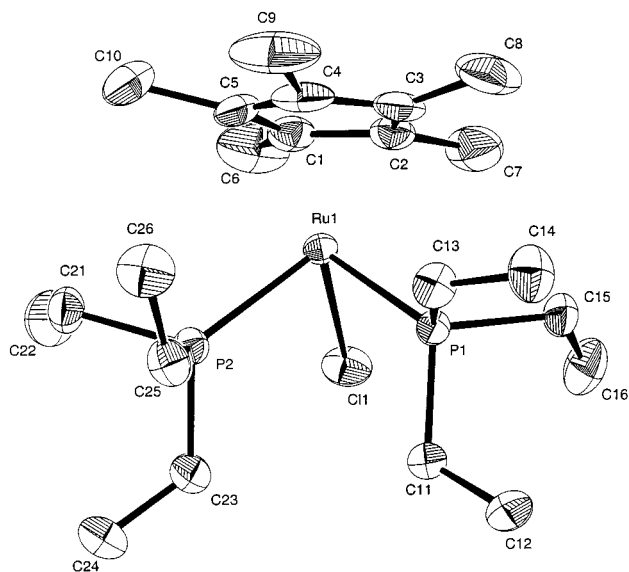
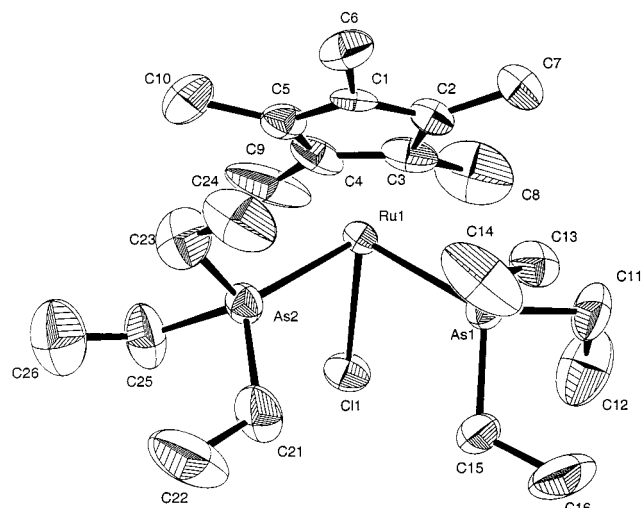
substitution (-32.2, -31.8, -29.4, -22.9 kcal/mol). However, a dissimilar trend is observed between the Ru–Cp*(centroid) distances, where **1** < **3** < **4** < **2**, and this trend does not correlate with enthalpy data. As expected, the P(1)–Ru–P(2) angle is the smallest (91.08°) in **1** and the largest in **4** (96.8°). Interestingly, the P(1)–Ru–P(2) angle does not correlate with the cone angle of the phosphine ligand for **2** and **3**. The P(1)–Ru–P(2) angle is slightly larger in **2** (94.5°) than in **3** (93.0°), even though the cone angle of PMe_2Ph (122°) is much smaller than that of PMePh_2 (136°).⁶

(7) In the course of the revision of this paper we became aware of the determination of **4** by Professor Paz-Sandoval's group: Guzei, I. A.; Paz-Sandoval, M. A.; Torres-Lubian, R.; Juarez-Saavedra, P. *Acta Crystallogr., Sect. C*, submitted for publication.

Table 2. Selected Bond Lengths and Angles in the Inner Coordination Sphere of the Complexes Cp*Ru(L)₂Cl^a

	1	2	3	4	5	6 ^b	7	8
Ru–P, Å	2.2923(9)	2.297(1)	2.2986(10)	2.3379(6)	2.3097(9)	2.442(1)	2.346(1)	2.2811(9)
Ru–Cl, Å	2.3015(9)	2.451(2)	2.3213(9)	2.3464(5)	2.3318(9)	2.449(1)	2.338(1)	2.2865(9)
Ru–Cp*, Å	1.860(3)	1.896(5)	1.872(3)	1.890(3)	1.880(3)	1.810(8)	1.871(4)	1.837(3)
cone angle, deg	118	122	136	145	132	128	132	NA
P–Ru–P, deg	91.08(3)	94.5(2)	93.02(3)	96.8(1)	92.8(1)	98.1(3)	100.1(2)	70.8(2)
P(1)–Ru–Cl, deg	85.30(3)	89.62(5)	86.8(1)	87.9(1)	90.5(1)	85.4(2)	86.3(1)	86.0(1)
P(2)–Ru–Cl, deg	91.54(3)	89.62(5)	94.04(3)	93.4(1)	88.2(1)	83.7(2)	88.6(1)	86.0(1)
Cp*–Ru–P(1), deg	127.0(1)	125.4(2)	129.7(1)	126.4(1)	125.2(1)	127.0(2)	126.0(1)	135.9(1)
Cp*–Ru–P(2), deg	128.0(1)	125.4(2)	124.9(1)	125.2(1)	130.8(1)	125.7(2)	124.7(1)	135.5(1)

^a Complete structural details are provided as Supporting Information. ^b Parameters referring to P represent As in this complex.

**Figure 5.** ORTEP diagram of Cp*Ru(P(Et)₃)₂Cl (**5**) with ellipsoids drawn at 30% probability.**Figure 6.** ORTEP diagram of Cp*Ru(AsEt₃)₂Cl (**6**) with ellipsoids drawn at 30% probability.

Solid-State Structures of Cp*Ru(P(Et)₃)₂Cl (5**) and Cp*Ru(AsEt₃)₂Cl (**6**).** Compounds **5** and **6** differ only in the pnictide atom in the EEt₃ ligand (E = As, P). The structures of **5** and **6** are similar: both are monoclinic and crystallize in the same space group (No. 14), although with different settings (*P*2₁/*c* and *P*2₁/*n*, respectively). The ORTEP depictions of **5** and **6** are respectively given in Figures 5 and 6. As expected, the average Ru–E distance is longer for E = As (2.446 Å) than for E = P (2.321 Å) and similarly the Ru–Cl

distance is longer in **6** (2.478 Å) than in **5** (2.456 Å). These structural features reflect the larger size of As vs P and the greater steric bulk of the triethylarsine ligand compared to the triethylphosphine ligand. This increased steric bulk can also be seen in the E–Ru–E angles of each, with the arsine angle (98.1°) greater than that of the phosphine (92.8°). Interestingly, the cone angles for these two ligands, while similar (128° for As, 132° for P), would lead one to predict the opposite trend for the E–Ru–E angles. Electronic factors must also be at play here. While the Ru–Cl distance in **5** is 0.022 Å shorter than in **6**, the Ru–Cp*(centroid) distances differ by nearly 0.07 Å, where the phosphine complex **5** displays a longer distance (1.880 Å) than the arsine complex **6** (1.811 Å). This donor trend is consistent with the current understanding of electronic contributions from these ligands.⁵ Enthalpy measurements reveal that triethylarsine complex **6** forms a less stable complex ($\Delta H_{\text{rxn}} = -15.0$ kcal/mol vs -27.2 kcal/mol for the triethylphosphine complex **5**). Thus, **6** is a poorer donor, permitting the Cp* ligand to donate more electron density to the metal, which is consistent with the shorter Ru–Cp*(centroid) distance found in **6** (1.811 Å) compared to that found in **5** (1.880 Å). These structural features are quite similar to those of the analogous CpRuCl(EEt₃)₂ complexes that have been previously reported.⁸

Solid-State Structures of Cp*Ru(PⁿBu₃)₂Cl (7**) and Cp*Ru(dmpm)Cl (**8**).** The organoruthenium complex **7** crystallizes in the monoclinic space group *P*2₁/*c* (No. 14) and has four molecules per unit cell. The ORTEP depictions of **7** and **8** are respectively given in Figures 7 and 8. Complexes **1**, **5**, and **7** differ in the types of alkyl substituents (Me, Et, ⁿBu). As expected, comparison of the Ru–P bond lengths of **1**, **5**, and **7** finds that the trimethylphosphine ligand in **1** has a shorter average Ru–P bond length (2.2969 Å) and is thermodynamically more stable (-32.2 kcal/mol) than either the triethylphosphine complex **5** (2.320 Å and -27.2 kcal/mol) or the tri-*n*-butylphosphine complex **7** (2.342 Å and -26.0 kcal/mol). However, a different trend is observed between the Ru–Cp*(centroid) distances, where **1** < **7** < **5**, which does not correlate with enthalpy data. The P(1)–Ru–P(2) bond angles (91.08° for **1**; 92.8° for **5**; 100.1° for **7**) in this case follow the trends expected from the cone angles (118° for the smaller PMe₃ versus 132° for both the bulkier PET₃ and PⁿBu₃ ligands).⁶

Cp*Ru(dmpm)Cl (**8**) crystallizes in the orthorhombic space group *Pbca* (No. 61), with one molecule in the

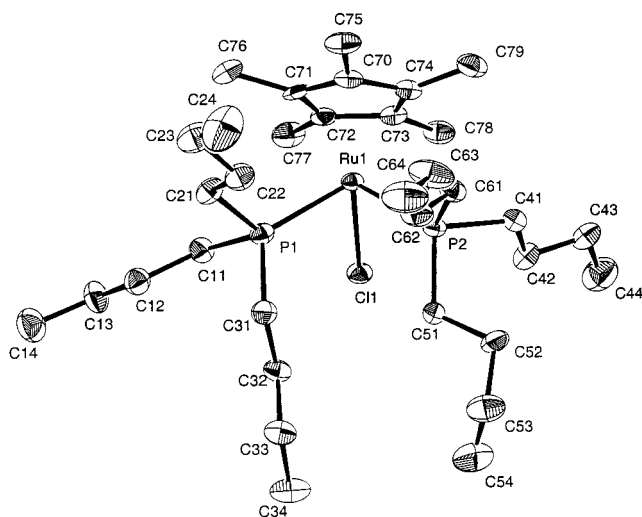


Figure 7. ORTEP diagram of $\text{Cp}^*\text{Ru}(\text{P}^n\text{Bu}_3)_2\text{Cl}$ (**7**) with ellipsoids drawn at 30% probability.

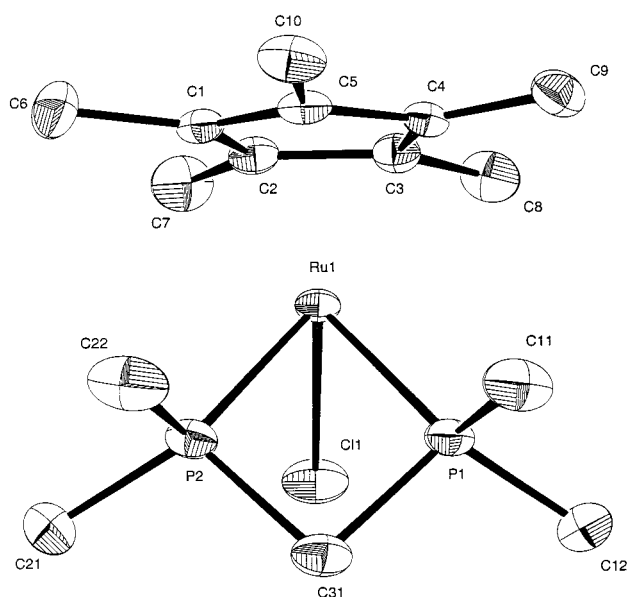


Figure 8. ORTEP diagram of $\text{Cp}^*\text{Ru}(\text{dmpm})\text{Cl}$ (**8**) with ellipsoids drawn at 30% probability.

asymmetric unit and eight in the unit cell. Apparently, **8** is more stable (-33.8 kcal/mol) than $\text{Cp}^*\text{Ru}(\text{PMe}_3)_2\text{Cl}$ (**1**) (-32.2 kcal/mol); this greater stability is reflected in the average Ru–P bond distance in **8** (2.284 Å), which is shorter than the average Ru–P distance in **1** (2.297 Å). Ring strain reflecting the constricted “bite”⁹ of the chelating dmpm is obvious from the distorted P(1)–C(31)–P(2) angle within the ligand of 91.6° and the small P(1)–Ru–P(2) angle of 70.8° .

Correlation Between Structural Parameters and Solution Calorimetric Data for $\text{Cp}^*\text{Ru}(\text{PR}_3)_2\text{Cl}$ Complexes. We have already seen in organoruthenium,² organorhodium,³ and organoiron⁴ tertiary phosphine and arsine based systems that steric, electronic, and structural parameters such as the Tolman⁶ cone angle (θ) and electronic parameter (χ) and metal–ligand bond lengths can be fitted to linear correlations involving solution thermochemical data. These correlations

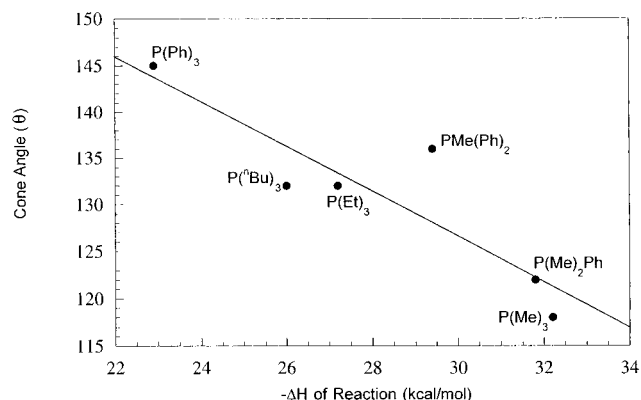


Figure 9. Plot of the cone angle (θ) versus the $-\Delta H$ values of reaction (kcal/mol) for the $\text{Cp}^*\text{Ru}(\text{L})_2\text{Cl}$ complexes (slope -2.42 ; $R = 0.893$).

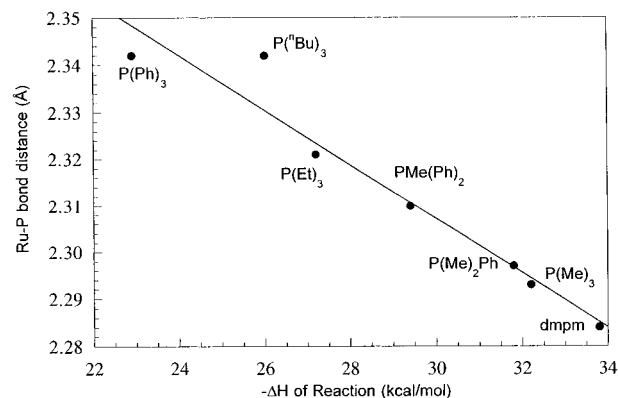


Figure 10. Plot of the Ru–P bond distance (Å) versus the $-\Delta H$ values of reaction (kcal/mol) for the $\text{Cp}^*\text{Ru}(\text{L})_2\text{Cl}$ complexes (slope -2.48 ; $R = 0.971$).

can be used to indicate the relative contribution of steric and electronic effects in these transition-metal systems.

Our previous work has examined a number of systems involving ruthenium, and we have been able to measure the enthalpies of reaction for these $\text{Cp}^*\text{Ru}(\text{PR}_3)_2\text{Cl}$ complexes, thereby determining the order of stability of complexes formed.⁵ For bond lengths of the inner coordination sphere of the $\text{Cp}^*\text{Ru}(\text{L})_2\text{Cl}$ complexes, no substantial correlation was found between the Ru–Cl bond lengths and the enthalpy of reaction. In fact, the Ru–Cl bond distance varies only slightly (2.453 ± 0.002 Å) over the range of P-ligand complexes **1–5**, **7**, and **8**. Additionally, no correlation was found between the Ru–Cp* (centroid) distance and the enthalpy of reaction. A straightforward relationship, as illustrated in Figure 9, appears to exist between the cone angle and the enthalpy of ligand substitution, with smaller ligands forming the most stable complexes. As shown in Figure 10, however, a higher degree of correlation exists between the reaction enthalpies and the Ru–P bond distances. The Ru–P bond length data used in this and associated relationships are the average of the two Ru–P bond lengths found in each complex. The reaction enthalpies involved in this correlation are directly related to Ru–P bond dissociation enthalpies, Figure 10 is in fact a bond length–relative bond dissociation enthalpy correlation.¹⁰ It is noteworthy that this relationship between the reaction enthalpies and the Ru–P bond distances appears insensitive to substituents and holds for triaryl, trialkyl, or mixed phosphines, and even

(9) Casey, C. P.; Whiteker, G. T.; Campana, C. F.; Powell, D. R. *Inorg. Chem.* **1990**, *29*, 3376–3381.

Table 3. Crystallographic Data for the Complexes Cp*Ru(L)₂Cl

	1	2	3	4	5	6 ^b	7	8
formula	C ₁₆ H ₃₃ ClP ₂ Ru	C ₂₆ H ₃₇ ClP ₂ Ru	C ₃₆ H ₄₁ ClP ₂ Ru	C ₄₆ H ₄₅ ClP ₂ Ru	C ₂₂ H ₄₅ ClP ₂ Ru	C ₂₂ H ₄₅ ClAs ₂ Ru	C ₃₄ H ₆₉ ClP ₂ Ru	C ₁₅ H ₂₉ ClP ₂ Ru
fw	423.94	548.08	672.22	796.37	508.10	595.99	676.43	407.90
color	orange	orange	orange	red-orange	red-orange	orange	orange	orange
space group ^a	<i>Pcba</i> (61)	<i>Cmc2₁</i> (36)	<i>P2₁/c</i> (14)	<i>P2₁/c</i> (14)	<i>P2₁/c</i> (14)	<i>P2₁/n</i> (14)	<i>P2₁/c</i> (14)	<i>Pcba</i> (61)
<i>a</i> , Å	15.510(4)	15.749(3)	10.254(1)	17.166(1)	15.252(4)	10.683(3)	14.588(3)	13.933(2)
<i>b</i> , Å	15.634(2)	12.719(3)	18.584(2)	10.726(1)	10.403(3)	15.987(4)	15.987(4)	15.7381(9)
<i>c</i> , Å	16.345(3)	13.080(3)	17.163(3)	20.603(1)	15.751(4)	15.796(4)	16.099(4)	16.678(2)
β, deg	90	90	100.73(1)	101.64(1)	97.73(1)	106.91(2)	92.40(2)	90
formula units/cell	8	4	4	4	4	4	4	8
<i>R</i> ^b	0.032	0.036	0.034	0.030	0.030	0.044	0.052	0.026
<i>R</i> _w ^b	0.031	0.037	0.032	0.037	0.030	0.037	0.049	0.030
error of fit	1.14	1.39	1.05	2.11	1.13	1.16	1.60	1.24

^a The number given in parentheses is the space group number from the *International Tables of X-Ray Crystallography*. ^b $R = \sum(|F_o| - |F_c|) / \sum |F_o|$; $R_w = \sum w(|F_o| - |F_c|)^2 / \sum w|F_o|^2$.

for the bidentate phosphine ligand dmpm, despite the clearly different nature of the latter. The correlation between crystalline Ru–P distances and solution thermochemical measurements suggests that longer bonds are associated with less exothermic reactions. This trend (dmpm > PMe₃ > PPhMe₂ > PPh₂Me > PETe₃ > PⁿBu₃ > PPh₃) can be explained in terms of the steric and electronic contributions of the donor P-ligands.⁶

While there are no other significant correlations between the enthalpy of reaction and structural parameters, as can be expected, there is a correlation between the P(1)–Ru–P(2) angle and the average P–Ru–Cp*-(centroid) angle. The P(1)–Ru–P(2) angle can be used as a measure of the steric bulk of the pnictide ligands, with a greater angle expected as the ligand occupies more space. Thus, as the P(1)–Ru–P(2) angle and the distance between the P atoms increases, the pnictide ligands move closer to the Cp* group. This in turn causes the average P–Ru–Cp*-(centroid) angle (and the distance between the pnictide ligands and the Cp*-(centroid)) to decrease as the Cp* and P-ligands move closer together.

Conclusion

Single-crystal X-ray diffraction studies of several Cp*Ru(ER₃)₂Cl systems have been performed in order to correlate structural parameters with enthalpies of ligand substitution. Among this series of complexes, reaction enthalpies correlate well with Ru–P bond distances but somewhat weakly with phosphine cone angle. Other relationships are not as straightforward, pointing out that various other factors (e.g., electronic or reorganizational) may also be operative and that they influence the structural chemistry and thermochemistry of this system in different ways.¹¹

Experimental Section

General Considerations. All manipulations involving organoruthenium complexes were performed under an inert atmosphere of argon or nitrogen, using standard high-vacuum or Schlenk techniques, or in a MBraun glovebox containing

less than 1 ppm of oxygen and water. The thermochemical data have been previously reported.⁵

Complexes **1–8** and Cp*Ru(COD)Cl were synthesized according to literature methods.^{5,12} A general procedure involved charging a flask with Cp*Ru(COD)Cl, an excess of ligand, and dry THF as solvent. After the mixture was stirred for about 2 h, the solvent was removed under vacuum. Hexane was vacuum-transferred to the cooled (–78 °C) flask; the solution was then warmed to room temperature, stirred, and then filtered. The solution was then cooled to –78 °C very slowly. After overnight cooling, cold filtration yielded single crystals of suitable quality for X-ray diffraction study.

Structure Determination and Crystallographic Data.

Crystallographic information for all complexes, including cell dimensions and details of the data collection, are given in Table 3. For each compound, a suitable crystal was mounted on the glass fiber of a goniometer head in a random orientation and placed in the cold stream of N₂ in an automated diffractometer using Mo Kα radiation. The cell dimensions were determined in each case from at least 25 centered reflections, and data were collected. Standard reflections were monitored during data collection. For complexes **2**, **4**, **5**, and **6** an azimuthal absorption correction was applied.

The structures were solved by direct methods using either the SHELXS or MULTAN programs. Each structure was refined in a full-matrix least-squares refinement on *F*, using anomalous terms for Ru, Cl, and As or P, with all non-hydrogen atoms refined anisotropically. In each case, hydrogen atoms were located from a Fourier difference map and used as the basis of H atom positions in the final structure. While the H atoms in **8** were able to be refined, all the other structures have idealized and fixed H atoms, after attempts to refine them proved unsatisfactory. ORTEP diagrams of each structure are given in Figures 1–8. Selected bond distances and angles are given in Table 2. Positional and equivalent isotropic parameters for all non-hydrogen atoms are given as Supporting Information.

Acknowledgment. S.P.N. acknowledges the National Science Foundation and DuPont (Educational Aid Grant) for financial support of this research.

Supporting Information Available: Details of the crystal structure determinations for complexes **1–8**. This material is available free of charge via the Internet at <http://pubs.acs.org>.

OM990090K

(10) For the description of such relationships see for example: Burrow, R. A.; Farrar, D. H.; Hao, J. B.; Lough, A.; Mourad, O.; Poe, A. J.; Zheng, Y. *Polyhedron* **1998**, *17*, 2907–2919 and references cited therein.

(11) Huang, J.; Haar, C. H.; Nolan, S. P.; Marshall, W. J.; Moloy, K. G. *J. Am. Chem. Soc.* **1998**, *120*, 7806–7815.

(12) Fagan, P. J.; Mahoney, W. S.; Calabrese, J. C.; Williams, I. D. *Organometallics* **1990**, *9*, 1843–1852.